FOCUSED ISSUE FEATURE

Advanced Filter Synthesis

Richard J. Cameron

Until the early 1970s, nearly all filter synthesis techniques were based on the extraction of electrical elements (lumped capacitors and inductors, transmission line lengths) from the polynomials that represented the filter's electrical performance in mathematical terms. This was perfectly adequate for the technologies and applications that were available at the time, and many important contributions were made to the art of advanced filter transfer and reflection polynomial generation, and then their conversion to electrical component values corresponding to the filter technologies that were available at this time [1]–[13].

In the early 1970s a revolution in telecommunication systems and available technology was taking place. The first satellite telecommunication systems were in operation and demand for their services was growing enormously, meaning that the ratio-frequency (RF) spectrum allocated to satellite communication systems had to be pushed to higher

Richard J. Cameron (richard.cameron@comdev.co.uk) is with Canopus Consultancy.

Digital Object Identifier 10.1109/MMM.2011.942007
Date of publication: 7 September 2011

 1527-3342/11/$26.00©2011 IEEE

frequency bands to accommodate the increasing volumes of traffic. The technology available to implement the components of these higher-frequency systems was also advancing, for example, better front-end low-noise amplifiers, high-power transmit amplifiers, antenna systems, and passive channelizing equipment. Also, the crowding of the available spectrum meant that the specifications on channel filters in terms of in-band linearity (group delay, insertion loss) and out-of-band selectivity (high close-to-band rejection and, for transmit filters, lowest possible insertion loss), were getting more demanding.

During this period, two important advances were made in the field of filter design to address the new demands. The first was the development of the design methods for advanced filtering functions incorporating built-in transmission zeros (TZs) and group delay features aimed particularly at microwave filter implementation. Then the introduction of the reflex (sometimes called the "folded") cross-coupled microwave filter [14]–[16], which allowed inter-resonator couplings, other than the usual main-line couplings between sequentially numbered resonators, to be implemented. These cross-couplings, as they came to be known, enabled the realization of special features of a filtering function, namely TZs to give a high close-to-band rejection of RF noise and interference, or linearization of in-band group delay, or both within the same filter structure.

The other major advance about this time was the development of dual-mode technology for waveguide filters at ComSat Laboratories [17]–[20] in response to very stringent performance requirements being imposed on spaceborne microwave equipment by the system designers. The innovation came in two parts—1) the development of the coupling matrix method for the holistic design of the filter's main and cross-coupling elements and 2) the propagating dual-mode waveguide configuration, which inherently provided the cross-couplings necessary for the realization of the special performance features without the need for complex and sensitive coupling elements.

The classic procedure for calculating the values of the coupling elements and resonant frequencies for the prototype filter

In the early 1970s a revolution in telecommunication systems and available technology was taking place. The first satellite telecommunication systems were in operation and demand for their services was growing enormously.

network, which forms the basis of the microwave filter design, involves first generating the polynomials, which represent the transfer and reflection characteristics (S_{21} and S_{11}), required from the network in order to satisfy the specifications. Then the prototype elements (capacitors, inductors, lengths of transmission line) are extracted from the polynomials. As the network is built up element by element, the polynomials decrease in degree until, when the network is fully synthesized, the coefficients of the polynomials are all zero apart from some constants. Different extraction strategies are required to obtain the specific topology of the prototype network that corresponds to the electrical components available in the technology it is intended to realize the microwave filter with.

The coupling matrix network synthesis method provides an alternative to the extraction of electrical elements one by one. The coupling matrix is simply a representation of the network, which may be used for the initial design, then the tuning, modelling and analysis of microwave filter performance. One important feature is the one-to-one correspondence between the elements of the coupling matrix and the individual physical components of the filter. Although the initial design of a filter network (the prototype network) assumes frequency-independent coupling elements and lossless and dispersionless resonators, these real-world effects may be accommodated when analyzing the matrix for filter performance prediction. Different characteristics may be allocated to different elements if there is a mix of technologies within the filter. Another advantage is the ability to reconfigure the coupling matrix through similarity transforms to arrive at a different coupling arrangement, corresponding to the available coupling elements of the particular microwave structure selected for the application. This can be done without going right back to the beginning of the network synthesis process to start again on a different network synthesis route, as would have to be done if the classical element extraction method was being used. More recently, coupling matrix synthesis theory has been advanced to include asymmetric filtering characteristics, which have become important for terrestrial telecommunication systems, particularly mobile telephony systems.

Because of the prevalence of the coupling matrix in microwave filter design, this article will concentrate on techniques for the synthesis and then the reconfiguration of the coupling matrix, ready for realization in a variety of microwave structures. Firstly the method for the generation of advanced polynomial filtering functions will be briefly outlined, followed by the synthesis of one of the canonical networks—the transversal matrix. Then the reconfiguration of the transversal matrix into various forms for realization in a variety of microwave structures will be discussed. Some examples are given to clarify certain aspects of the design processes, and references cited if further information is required by the reader.

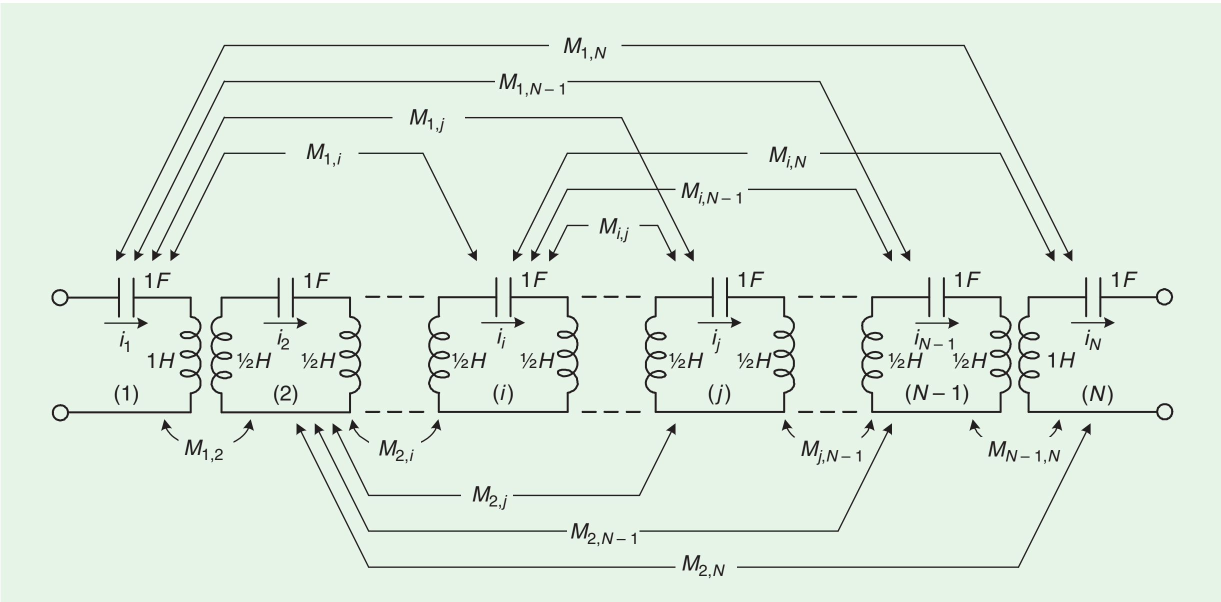

Figure 1. *Multicoupled network—classical bandpass prototype representation (courtesy of A.E. Atia).*

The coupling matrix network synthesis method provides an alternative to the extraction of electrical elements one by one.

The Coupling Matrix

The basic circuit model that was used in [20] was a bandpass prototype which is a generalized multicoupled network as shown in Figure 1. The circuit comprises a cascade of lumped element series resonators intercoupled through transformers; each resonator comprising a capacitor of 1 Farad in series with the self inductances of the main-line transformers, which total 1 Henry within each loop. This gives a centre frequency of 1 radian/second, and the couplings are normalized to give a bandwidth of 1 rad/sec. In addition every loop is theoretically coupled to every other loop through cross-mutual couplings between the main-line transformers.

This network may be represented by an $N \times N$ coupling matrix where N is the number of resonators (the degree or order) of the filter. The elements of the matrix contain the values of the couplings between each of the resonators; between sequentially numbered resonator nodes (main-line couplings), and nonadjacent nodes (cross-couplings). Because the electrical elements of the network are passive and reciprocal, the matrix is symmetrical about its principal diagonal. To more closely represent a microwave circuit, the transformers may be replaced by immittance inverters (90° lengths of transmission line), which approximate the electrical characteristics of many microwave coupling devices. By placing an inverter at each end of the network, the input and output couplings of the filter may also be represented (Figure 2). With the extra inverters, the matrix increases to $N+2 \times N+2$ in size—the so-called $N+2$ coupling matrix—and becomes the dual network of Figure 1.

The circuit in Figure 1 will only support symmetric filtering characteristics, but with the addition of a series-connected frequency-invariant reactance (FIR) within each loop, the capability of the circuit may be extended to include asymmetric cases (see Figure 2). These have been finding increasing application recently, as the RF frequency spectrum becomes more crowded and rejection specifications more severe. The FIR (sometimes referred to as a self-coupling) represents a frequency offset of the resonator it is associated with, and its value is entered along the diagonal of the coupling matrix. Because the inverters are also frequency-invariant and there are no self-inductors, the network of Figure 2 may now be considered as a low-pass prototype, which simplifies the synthesis process somewhat.

The $N+2$ short-circuit admittance matrix $[y']$ for the network of Figure 2 may be separated out into its purely resistive and purely reactive parts:

$$[y'] = [\mathbf{G}] + [j\mathbf{M} + \mathbf{U}] = [\mathbf{G}] + [y] \qquad (1)$$

where the purely real matrix $[\mathbf{G}]$ contains the conductive terminations G_S and G_L of the network and the purely reactive admittance $[y] = [j\mathbf{M} + \mathbf{U}]$ is the sum of the coupling matrix $\mathbf{M}$ and the diagonal matrix $\mathbf{U}$ which contains the frequency variable $s\ (= j\omega)$, except for U_{SS} and U_{LL} which are zero.

The $N+2$ coupling matrix $[\mathbf{M}]$ contains the values of all the couplings in the network including the input/output couplings (which may connect to internal resonators as well as the first and Nth). The

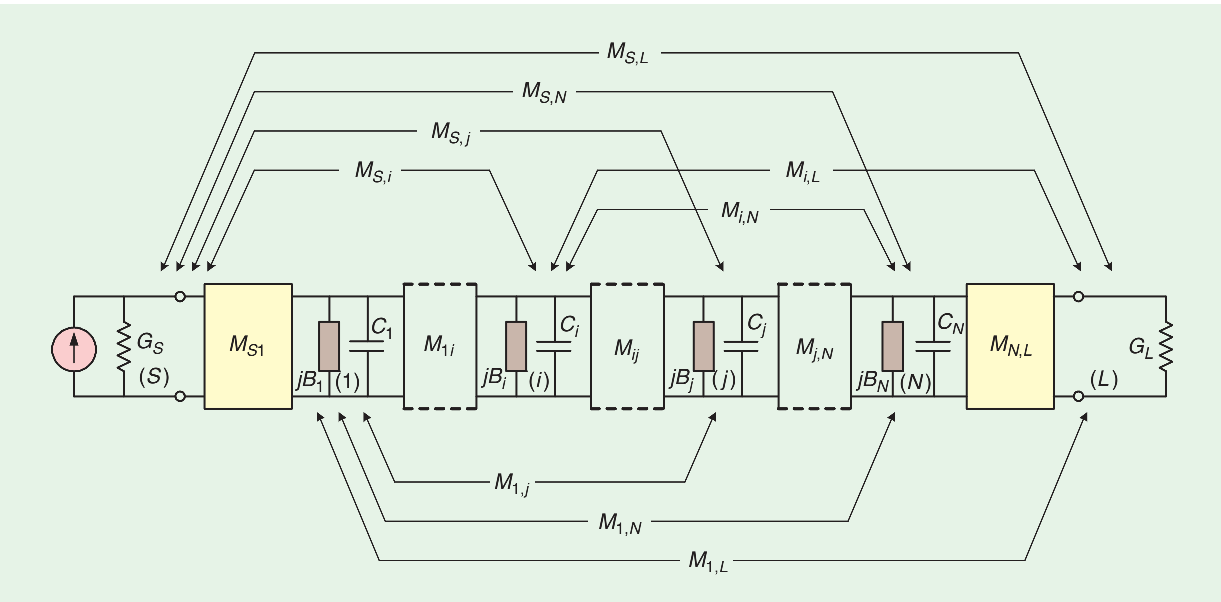

Figure 2. *Multicoupled network—equivalent low-pass prototype modified to include FIRs and immittance inverters. (Reprinted with permission from [22].)*

The filter design process begins with the generation of the rational polynomials embodying the transfer and reflection characteristics.

diagonal contains the values of the frequency invariant reactances which represent resonator frequency offsets (the negative values of the FIRs in Figure 2), which are necessary for asymmetric characteristics. Figure 3(a) shows a canonical coupling matrix which has all couplings present, and Figure 3(b) an example of a typical coupling and routing diagram, representing a possible inter-resonator coupling arrangement.

Synthesis Procedure

The filter design process begins with the generation of the rational polynomials embodying the transfer and reflection characteristics S_{21} and S_{11}, which satisfy the rejection and in-band specifications of the application. Once these have been obtained, the next step in the process is to synthesize the coupling matrix

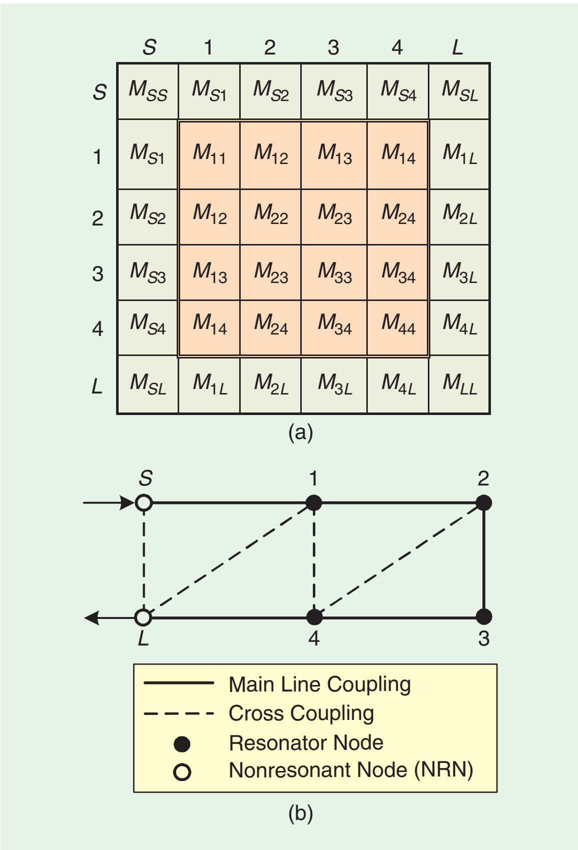

Figure 3. *(a) Fourth degree N+2 coupling matrix with all possible couplings. The core N×N matrix is indicated within the double lines. (b) An example of a coupling and routing diagram representing the coupling matrix of a fourth degree fully canonical network in cross-coupled folded configuration. (Reprinted with permission from [22].)*

and configure it such that its nonzero entries coincide with the available coupling elements of the structure it is intended to use for realizing the filter response. Finally, the dimensions of the coupling elements are calculated from the coupling matrix values.

The procedure is illustrated in Figure 4 for a sixth-degree characteristic with two TZs and realized in coupled waveguide resonator technology. The direct correspondence between the elements of the coupling matrix and the physical filter components is highlighted.

Generation of Transfer and Reflection Polynomials

In modern telecommunication, radar and broadcast systems, where the allocated RF frequency spectrum has become very congested, the specifications on performance from the component microwave filters have become increasingly stringent. For these applications the Chebyshev class of filtering characteristic is very suitable on account of the inherent equiripple in-band return loss level and the ability to build in TZs to provide high close-to-band rejection levels or in-band group delay equalization, or both within the same filtering function. Moreover, the TZs may be placed asymmetrically to optimally comply with asymmetric specifications. A method for generating the low-pass prototype polynomials for the Chebyshev class of filter function is outlined below.

For any two-port lossless filter network composed of a series of N intercoupled resonators, the transfer and reflection functions may be expressed as a ratio of two polynomials [21]:

$$S_{11}(\omega) = \frac{F(\omega)/\varepsilon_R}{E(\omega)} \qquad S_{21}(\omega) = \frac{P(\omega)/\varepsilon}{E(\omega)}, \tag{2}$$

where

$$\varepsilon = \frac{1}{\sqrt{1 - 10^{-RL/10}}} \left| \frac{P(\omega)}{E(\omega)} \right|_{s=\pm j},$$

and $\varepsilon_R = 1$ or $\varepsilon_R = \varepsilon/\sqrt{\varepsilon^2 - 1}$ if the function is fully canonical, and RL is the prescribed equiripple return loss level of the Chebyshev function in decibles. $S_{11}(\omega)$ and $S_{21}(\omega)$ share a common denominator $E(\omega)$. The polynomials $E(\omega)$and $F(\omega)$ are both of degree $\mathbf{N}$ while the polynomial $P(\omega)$ carries the n_{fz} transfer function finite-position TZs. For a Chebyshev filtering function ε is a constant normalizing $S_{21}(\omega)$ to the equiripple level at $\omega = \pm 1$, and $\varepsilon_R = 1$ except for fully canonical filters (i.e., $n_{fz} = N$).

The ratio $C_N(\omega) = F(\omega)/P(\omega)$ is known as the "filtering function" of degree N, and its poles and zeros are the roots of $P(\omega)$ and $F(\omega)$, respectively. It has a form for the general Chebyshev characteristic [22]

$$C_N(\omega) = \cosh\left[\sum_{n=1}^{N} \cosh^{-1}(x_n(\omega))\right], \tag{3}$$

where

$$x_n(\omega) = \frac{1-\omega\omega_n}{\omega-\omega_n},$$

and ω_n are the positions of the n_{fz} finite-position TZs, and the remaining $N - n_{fz}$ zeros at $\omega = \pm\infty$.

For a prescribed set of TZs that make up the polynomial $P(\omega)$ and a given equiripple return loss level, the reflection numerator polynomial $F(\omega)$ may be built up with an efficient recursive technique, and then the polynomial $E(\omega)$ found from the conservation of energy principle [21]–[23].

An example of this synthesis method is given in [21] for a fourth-degree prototype with 22 dB return loss level and two imaginary axis TZs at $s = +j1.3217$ and $+j1.8082$ which are so positioned to give two rejection lobes at 30 dB each on the upper side of the passband. The polynomials and corresponding singularities of $P(s)$ $F(s)$ and $E(s)$ are given in Table 1, and plots of the transfer and rejection characteristic are shown in Figure 5

Coupling Matrix Generation

The second step in the synthesis procedure is to calculate the values of the coupling elements of a canonical coupling matrix from the transfer and reflection polynomials. Three forms of the canonical matrix are commonly used—the folded [16], arrow [25] or transversal [24]. The latter is particularly easy to synthesize, and the other two may be derived from it quite simply by applying a formal series of analytically calculated similarity transforms.

The transversal coupling matrix comprises a series of N individual first-degree low pass sections, connected

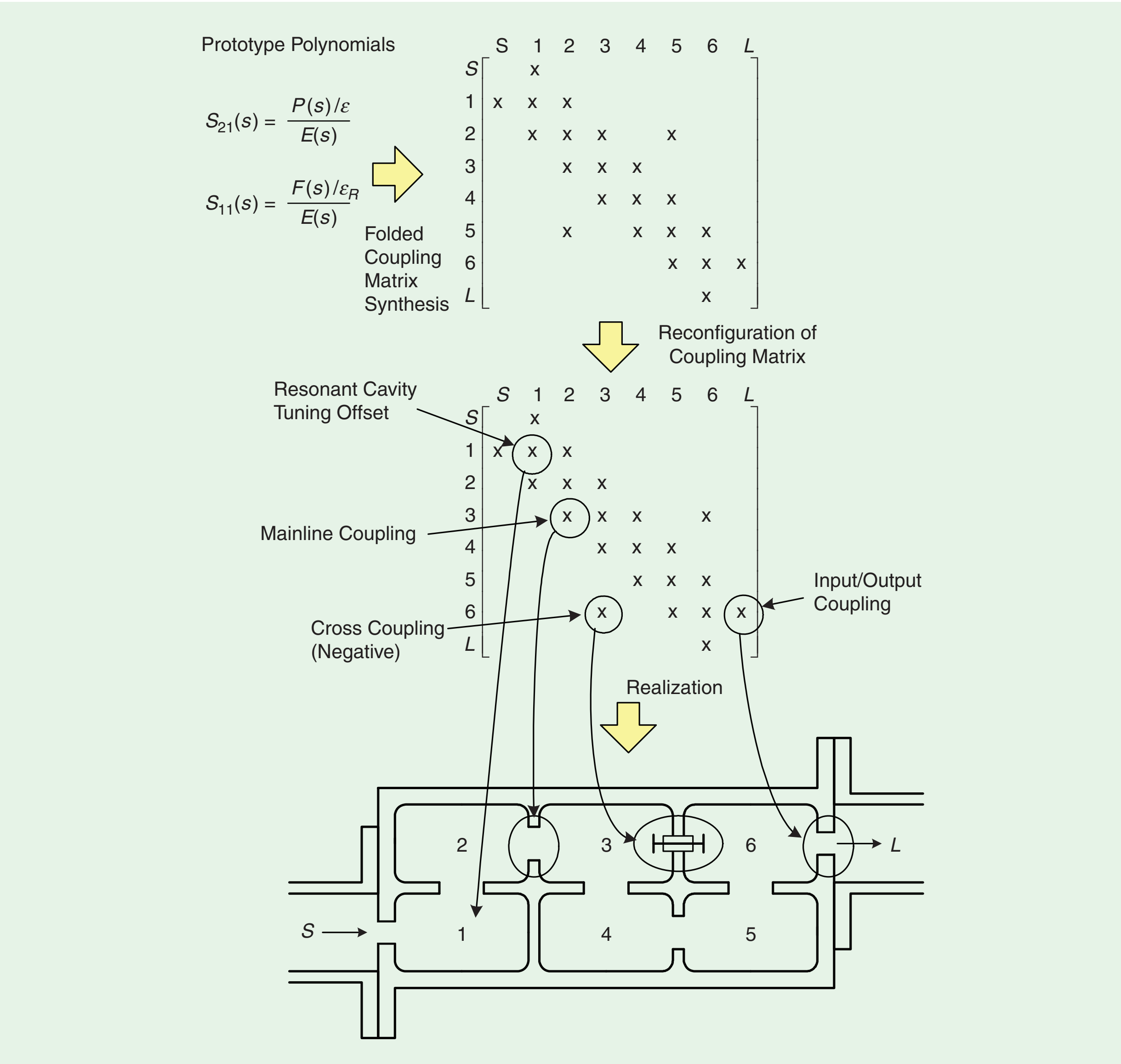

Figure 4. *Microwave filter design process—synthesis of the polynomials for the transfer and reflection function, synthesis of canonical coupling matrix, reconfiguration of coupling matrix, realization in microwave coupled-resonator technology. (Reprinted with permission from [22].)*

TABLE 1. 4–2 asymmetric Chebyshev filtering function with two prescribed transmission zeros.

Transfer and Reflection Function Polynomials.

s^i, i =	$E(s)$	$F(s)$	$P(s)$
0	$-0.1268 - j2.0658$	$+0.0208$	$-j2.3899$
1	$+2.4874 - j3.6255$	$-j0.5432$	$+3.1299$
2	$+3.6706 - j2.1950$	$+0.7869$	$j1.0$
3	$+2.4015 - j0.7591$	$-j0.7591$	
4	$+1.0$	$+1.0$	

Corresponding Singularities.

	Reflection Zeros (Roots of $F(s)$)	Transmission Zeros (Prescribed)	Transmission/Reflection Poles (Roots of $E(s)$)
1	$-j0.8593$	$+j1.3217$	$-0.7437 - j1.4178$
2	$-j0.0365$	$+j1.8082$	$-1.1031 + j0.1267$
3	$+j0.6845$	$j\infty$	$-0.4571 + j0.9526$
4	$+j0.9705$	$j\infty$	$-0.0977 + j1.0976$
	$\varepsilon_R = 1.0$	$\varepsilon = 1.1548$	

in parallel between the source and load terminations but not to each other [Figure 6(a)]. The direct source-load coupling inverter M_{SL} is included to allow fully canonical transfer functions to be realized, according to the minimum path rule, i.e., n_{fzmax}, the maximum number of finite position TZs that may be realized by the network $= N - n_{\min}$, where $n_{\min}$ is the number of resonator nodes in the shortest route through the couplings of the network between the source and load terminations. In fully canonical networks $n_{\min} = 0$ and so $n_{fzmax} = N$, the degree of the network.

Each of the N low-pass sections comprises one parallel-connected capacitor C_k and one frequency invariant susceptance B_k, connected through admittance inverters of characteristic admittances M_{Sk} and M_{Lk} to the source and load terminations, respectively. The circuit of the kth low-pass section is shown in Figure 6(b)

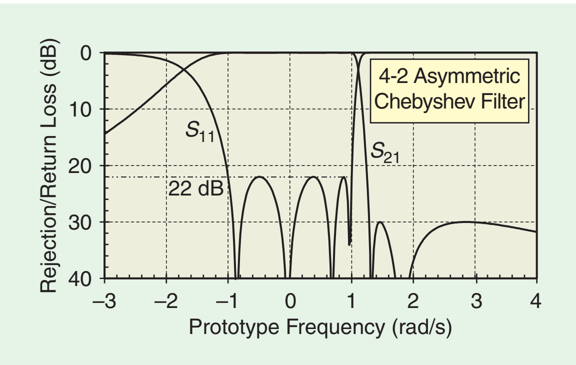

Figure 5. *Low-pass prototype transfer and reflection characteristics of the 4-2 asymmetric Chebyshev filter, with two prescribed transmission zeros at $s_1 = +j1.3217$ and $s_2 = +j1.8082$. (Reprinted with permission from [22].)*

The approach that is employed to synthesize the $N+2$ transversal coupling matrix is to construct the two-port short-circuit admittance parameter matrix $[Y_N]$ for the overall network in two ways; the first from the coefficients of the rational polynomials of the transfer and reflection scattering parameters $S_{21}(s)$ and $S_{11}(s)$ which represent the characteristics of the filter to be realized, and the second from the circuit elements of the transversal array network. By equating the $[Y_N]$ matrices as derived by these two methods, the elements of the coupling matrix associated with the transversal array network may be related to the coefficients of the $S_{21}(s)$ and $S_{11}(s)$ polynomials.

In [24] it is explained how the matrix $[Y_N]$ is built up very simply from the coefficients of the $E(\omega)$, $F(\omega)$ and $P(\omega)$ polynomials as derived in the previous section. From the coefficients, the eigenvalues λ_k and the associated residues r_{21k} and r_{22k}, $k = 1, 2, \ldots, N$ of the network may be found using partial fraction expansions, whereupon the expression for $[Y_N]$ in terms of the eigenvalues and residues may be built up:

$$[Y_N] = j\begin{bmatrix} 0 & K_\infty \\ K_\infty & 0 \end{bmatrix} + \sum_{k=1}^{N} \frac{1}{(s - j\lambda_k)} \cdot \begin{bmatrix} r_{11k} & r_{12k} \\ r_{21k} & r_{22k} \end{bmatrix}. \quad (4)$$

Secondly, the elements of each of the low-pass resonators in Figure 6(b) are cascaded (using ABCD matrices), converting these to the individual y-parameter matrices, and then adding them to form the overall $[Y_N]$ matrix in terms of the network elements

$$[Y_N] = j\begin{bmatrix} 0 & M_{SL} \\ M_{SL} & 0 \end{bmatrix} + \sum_{k=1}^{N} \frac{1}{(sC_k + jB_k)} \times \begin{bmatrix} M_{Sk}^2 & M_{Sk}M_{Lk} \\ M_{Sk}M_{Lk} & M_{Lk}^2 \end{bmatrix}. \quad (5)$$

Construction of the N+2 Transversal Matrix

Now the two expressions for $[Y_N]$, the first in terms of the residues r_{21k} and r_{22k} and the eigenvalues λ_k, which have already been derived from the S_{21} and S_{22} polynomials of the desired filtering function, and the second in terms of the circuit elements of the transversal array, may be equated. This leads to the following relationships between the residues and the transversal coupling matrix elements:

$$C_k = 1 \quad \text{and} \quad B_k\,(\equiv M_{kk}) = -\lambda_k$$
$$M_{SL} = K_\infty$$
$$M_{Lk}^2 = r_{22k} \quad \text{and} \quad M_{Sk}M_{Lk} = r_{21k}.$$

Therefore,

$$M_{Lk} = \sqrt{r_{22k}}$$

and

$$M_{Sk} = r_{21k}/\sqrt{r_{22k}} = \sqrt{r_{11k}} \qquad k = 1, 2, \ldots, N \qquad (6)$$

Because the capacitors C_k of the parallel networks are all unity, and the frequency-invariant susceptances B_k $(= -\lambda_k$, representing the self couplings $M_{11} \to M_{NN})$, the input couplings M_{Sk}, the output couplings M_{Lk}, and the direct source-load coupling M_{SL} are all now defined, the reciprocal $N+2$ transversal coupling matrix **M** representing the network in Figure 7 may now be constructed. M_{Sk} are the N input couplings, and they occupy the first row and column of the matrix from positions 1 to N (see Figure 7). Similarly M_{Lk} are the N output couplings and they occupy the last row and column of **M** from positions 1 to N. All other entries are zero.

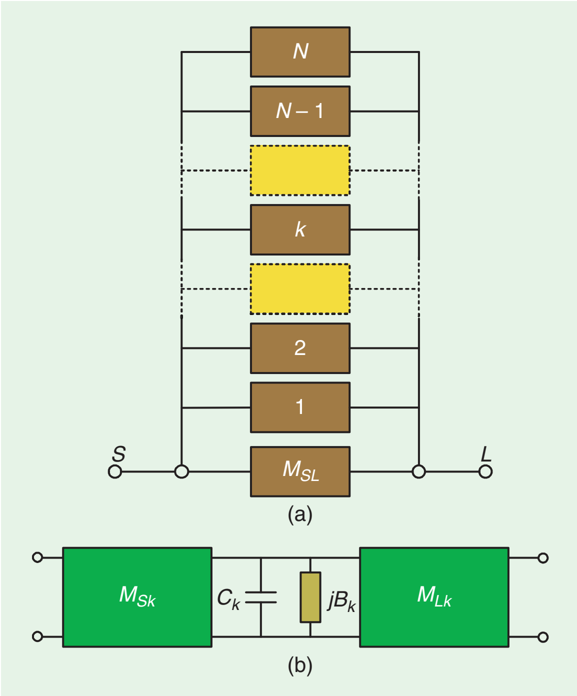

Figure 6. *Canonical transversal array. (a) N resonator transversal array including direct source-load coupling M_{SL}. (b) Equivalent circuit of the kth low-pass resonator in the transversal array. (Reprinted with permission from [22].)*

Similarity Transformation and Reconfiguration

The elements of the transversal coupling matrix that result from the synthesis procedure may be realized directly by the coupling elements of a filter structure if it is convenient to do so. However, for most coupled-resonator technologies, the couplings of the transversal matrix are physically impractical or impossible to realize. It becomes necessary to reconfigure the matrix with a sequence of similarity transforms (sometimes called rotations) [25], [26] until a more convenient coupling topology is obtained. The use of similarity transforms ensures that the eigenvalues and eigenvectors of the matrix **M** are preserved, such that under analysis the transformed matrix will yield exactly the same transfer and reflection characteristics as the original matrix.

There are several more practical canonical forms for the transformed coupling matrix **M**. Two of the better-known forms are the arrow form [25] and the more generally useful folded form [23], [27] (Figure 8). Either of these canonical forms may be used directly if it is convenient to realize the couplings, or be used as a starting point for the application of further transforms to create an alternative resonator intercoupling topology, optimally adapted for the physical and electrical constraints of the technology with which the filter will eventually be realized e.g., [28], [29]. The method for reduction of the coupling matrix to the folded form will be outlined here. The arrow form may be derived using a very similar method [22].

A similarity transform (or rotation) on an $N \times N$ coupling matrix $\mathbf{M}_0$ is carried out by pre- and post-multiplying $\mathbf{M}_0$ by an $N \times N$ rotation matrix **R** and its transpose $\mathbf{R}^t$ [26]:

	S	1	2	3	..	k	..	N – 1	N	L
S		M_{S1}	M_{S2}	M_{S3}	..	M_{Sk}	..	$M_{S,N-1}$	M_{SN}	M_{SL}
1	M_{1S}	M_{11}								M_{1L}
2	M_{2S}		M_{22}							M_{2L}
3	M_{3S}			M_{33}						M_{3L}
:	:				. .					:
k	M_{kS}					M_{kk}				M_{kL}
:	:						. .			:
N – 1	$M_{N-1,S}$							$M_{N-1,N-1}$		$M_{N-1,L}$
N	M_{NS}								M_{NN}	M_{NL}
L	M_{LS}	M_{L1}	M_{L2}	M_{L3}	..	M_{Lk}	..	$M_{L,N-1}$	M_{LN}	

Figure 7. *N+2 canonical coupling matrix **M** for the transversal array. The core N×N matrix is indicated within the double lines. The matrix is symmetric about the principal diagonal, i.e., $M_{ij} = M_{ji}$. (Reprinted with permission from [22].)*

	S	1	2	3	4	L
S	sc	m				sx
1	m	sc	m		sx	ax
2		m	sc	m	ax	
3			m	sc	m	
4		sx	ax	m	sc	m
L	sx	ax			m	sc

(a)

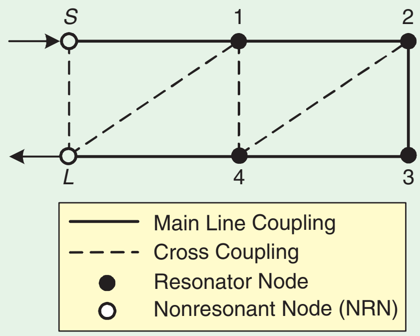

(b)

Figure 8. *$N+2$ folded canonical network, fourth degree example. (a) Coupling matrix: sc and ax couplings are generally zero for symmetric characteristics. (b) Coupling and routing schematic. Possible nonzero couplings: sc=self-coupling, m=main-line coupling, ax=asymmetric cross-coupling, and sx=symmetric cross-coupling. Couplings are equivalued about the principal diagonal.*

$$\mathbf{M}_1 = \mathbf{R}_1 \cdot \mathbf{M}_0 \cdot \mathbf{R}_1^t, \tag{7}$$

where $\mathbf{M}_0$ is the original matrix, $\mathbf{M}_1$ is the matrix after the transform operation, and the rotation matrix $\mathbf{R}$ is defined as in Figure 9. The pivot $[i, j]$ $(i \neq j)$ of $\mathbf{R}_r$ means that elements $R_{ii} = R_{jj} = \cos\theta_r$, $R_{ji} = -R_{ij} = \sin\theta_r$ $(i, j \neq \text{S or L})$, and θ_r is the angle of the rotation. The other principal diagonal entries are = 1 and all other off-diagonal entries are zero. The transpose $\mathbf{R}^t$ is the same as $\mathbf{R}$ except $R_{ij}^t = -R_{ji}^t = \sin\theta_r$.

	S	1	2	3	4	L
S	1					
1		1				
2			c_r		$-s_r$	
3				1		
4			s_r		c_r	
L						1

$c_r \equiv \cos\theta_r$, $s_r \equiv \sin\theta_r$

Figure 9. *Example of fourth degree rotation matrix $\mathbf{R}_r$: pivot [2, 4], angle θ_r.*

The eigenvalues of the matrix $\mathbf{M}_1$ after the transform are the same as those of the original matrix $\mathbf{M}_0$, which means that an arbitrarily long series of transforms with arbitrarily defined pivots and angles may be applied, starting with $\mathbf{M}_0$. Each transform in the series takes the form

$$\mathbf{M}_r = \mathbf{R}_r \cdot \mathbf{M}_{r-1} \cdot \mathbf{R}_r^t \quad r = 1, 2, 3, \cdots, R, \tag{8}$$

and, under analysis, the matrix $\mathbf{M}_R$ resultant at the end of the series of transforms will yield exactly the same performance as the original matrix $\mathbf{M}_0$. With an analytically calculated angle θ_r and judiciously chosen pivot positions, coupling elements may be zeroed (annihilated) and others created to arrive at a coupling matrix whose nonzero entries correspond to the available interresonator coupling elements of the filter structure it is intended to realize the required transfer and reflection characteristics with.

By applying a series of rotations, the $N+2$ transversal matrix may be reduced to the folded form. The pivots and a formula for calculating the angle of such a sequence is given below for a fourth-degree example, annihilating the elements M_{S4}, M_{S3}, M_{S2}, M_{2L}, M_{3L}, and finally M_{13} in sequence (see Table 2). The resulting folded configuration coupling and routing schematic is shown in Figure 8(b).

The final values and positions of the elements in the cross diagonals of the folded coupling matrix (the cross couplings) are automatically determined—no specific action to annihilate couplings within them needs to be taken if they are not needed to realize the particular transfer function under consideration.

In-Line (Propagating) Configurations

Although the folded coupling matrix may be realized directly with a microwave structure of some kind, e.g., coaxial or dielectric resonators, input/output isolation sometimes becomes a problem, particularly when operating the resonator in dual mode, i.e., two orthogonal resonances in the same physical cavity. Here small asymmetries in the resonator caused by tuning screws, for example, will limit the amount of far-out-of-band rejection that the filter can achieve, e.g., to about 25 dB in the case of Ku-band dual-mode cylindrical resonators.

For these structures it is usually better to reconfigure the folded coupling matrix into an in-line or propagating form, where the input and output are at opposite ends of the filter structure. In ref [22] some methods are given to reconfigure the folded matrix for an even-degree symmetric characteristic into an in-line form where the values of the coupling elements are symmetric about the physical centre of the filter, i.e., the coupling matrix is symmetric about both diagonals. However, these methods sometimes have restrictions on the pattern of TZs that can be realized and so a more general method is more often used. This involves a series of rotations, starting with the folded matrix, and with pivots and rotation angles for degrees 6, 8, and 10 as shown in Table 3. The sequences for degrees 12 and 14 may be found in refs. [29], [30], and odd degrees may be accommodated by using the next-lowest even degree, e.g., for a ninth-degree use the eighth-degree sequence.

Although the in-line topology of the asymmetric in-line realization is exactly the same as for the symmetric equivalent, the values of the in-line coupling matrix, and therefore the dimensions of the corresponding physical coupling elements, are not equal-valued about the physical centre of the structure [29]. Although this means more design effort to develop and manufacture a working filter, there is an advantage in that there are no restrictions on the pattern of TZs that the prototype may incorporate (apart from the usual conditions, i.e., the minimum path rule must be obeyed, and symmetry of the pattern of TZs about the imaginary axis (unitary condition), and about the real axis (symmetric characteristics) must be preserved). Moreover the computations required to produce the asymmetric in-line configuration are less complex. Figure 10(a) and (b) shows

TABLE 2. Fourth-degree example: pivots and angles of the similarity transform sequence for the reduction of the transversal (or any other) matrix to the folded configuration. Total number of transforms $R = \sum_{n=1}^{N-1} n = 6$.

Transform Number r	Pivot $[i, j]$	Element to be Annihilated in Matrix $\mathbf{M}_0$		$\theta_r = \tan^{-1}(cM_{kl}/M_{mn})$				
				k	l	m	n	c
1	[3, 4]	M_{S4}	in row S	S	4	S	3	−1
2	[2, 3]	M_{S3}	"	S	3	S	2	−1
3	[1, 2]	M_{S2}	"	S	2	S	1	−1
4	[2, 3]	M_{2L}	in column L	2	L	3	L	+1
5	[3, 4]	M_{3L}	"	3	L	4	L	+1
6	[2, 3]	M_{13}	in row 1	1	3	1	2	−1

Table 3. Pivot positions and rotation angles for the general asymmetric in-line realization, for degrees 6, 8, and 10.

Degree N	Rotation No. r	Pivot $[i, j]$	$\theta_r = \tan^{-1}(cM_{kl}/M_{mn})$				
			k	l	m	n	c
6	1	[2, 4]	2	5	4	5	+1
8	1	[4, 6]	3	6	3	4	−1
	2	[2, 4]	2	7	4	7	+1
	3	[3, 5]	2	5	2	3	−1
	4	[5, 7]	4	7	4	5	−1
10	1	[4, 6]	4	7	6	7	+1
	2	[6, 8]	3	8	3	6	−1
	3	[7, 9]	6	9	6	7	−1

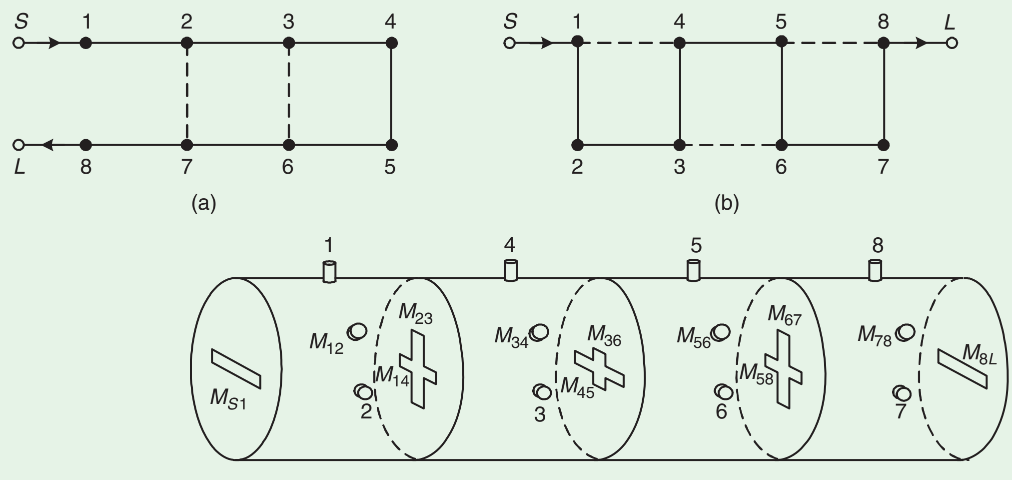

Physical Cavity No.		1	2	3	4
Containing Electrical Resonance Numbers	Vertical Polarization	1	4	5	8
	Horizontal Polarization	2	3	6	7

(c)

Figure 10. *Eighth-degree network: (a) cross-coupled folded configuration (b) after conversion to in-line topology. (c) Possible realization in cylindrical dual-mode cavities. (Reprinted with permission from [22].)*

For most coupled-resonator technologies, the couplings of the transversal matrix are physically impractical or impossible to realize.

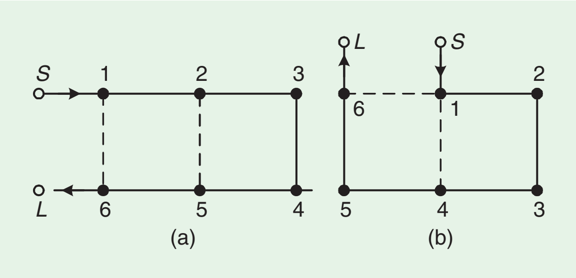

Figure 11. *Pfitzenmaier configuration—6-4 symmetric filtering characteristic. (a) Original folded configuration. (b) After transformation to Pfitzenmaier configuration. (Reprinted with permission from [22].)*

the reconfiguration of the coupling/routing diagram for an eight–four characteristic in folded form to an in-line form, and Figure 10(c) illustrates a possible realization in cylindrical dual-mode cavities.

Pfitzenmaier Configurations

Another configuration that is able to avoid the input/output isolation problem associated with the folded configuration in a dual-mode structure was introduced by Pfitzenmaier [31] for sixth-degree symmetric filtering characteristics. In [31] it is shown that the synthesized sixth-degree circuit can be transformed (not using coupling matrix methods) to a topology where the input and output resonances (1 and 6) are in adjacent cavities of the dual-mode structure, thereby avoiding the isolation problem. Furthermore, because it is possible to directly cross-couple resonances 1 and 6, the signal only has two resonances to pass through between the input and output, and therefore by the minimum path rule, the Pfitzenmaier configuration is able to realize $N-2$ TZs, the same as the folded structure. The coupling and routing diagram for a sixth-degree example is shown in Figure 11.

The Pfitzenmaier configuration may be easily obtained for any even degree symmetric characteristic ≥ 6 by using a sequence of coupling matrix rotations [28]. Unlike the asymmetric in-line realization, the pivots and angles of the rotations in the sequence may be defined with simple equations. Starting with the folded matrix, a series of $R = (N-4)/2$ rotations is applied according to (9) after which the Pfitzenmaier configuration is obtained.

For the rth rotation, pivot $=[i, j]$ and associated angle $=\theta_r$, where:

$$\left.\begin{aligned} i &= r+1 \\ j &= N-i \\ \theta_r &= \tan^{-1}(-M_{i,N-r}/M_{j,N-r}) \end{aligned}\right] r = 1, 2, 3, \ldots, R \quad (9)$$

and N is the degree of the filter ($N =$ even integer ≥ 6).

Advanced Configurations

In this section some advanced coupling matrix configurations will be considered. The first is the cul-de-sac configuration, which is derived from the folded coupling matrix, and has the principal advantage that it needs no diagonal cross couplings even if realizing asymmetric characteristics. The second is the cascaded trisection configuration which is derived from the arrow canonical matrix. This has applications for the generation of cascaded n-tuplets and box filters

The Cul-de-Sac Configuration

The cul-de-sac configuration [24], [32] in its basic form is restricted to double-terminated networks and will realize a maximum of $N-3$ TZs. Otherwise it will accommodate any even- or odd-degree symmetric or asymmetric prototype. Moreover its form lends itself to a certain amount of flexibility in the physical layout of its resonators.

A typical cul-de-sac configuration is shown in Figure 12(a) for a tenth-degree prototype which will accommodate a maximum of seven TZs. There is a central core of a quartet of resonators in a square formation [1, 2, 9, and 10 in Figure 12(a)], straight-coupled to each other (i.e., no diagonal cross-couplings). One of these couplings is always negative; the choice of which one is arbitrary. The entry to and exit from the core quartet are from opposite corners of the square [1 and 10, respectively, in Figure 12(a)].

Some or all of the rest of the resonators are strung out in cascade from the other two corners of the core quartet in equal numbers (even-degree prototypes) or one more than the other (odd degree prototypes). The last resonator in each of the two chains has no output coupling, hence the nomenclature cul-de-sac for this

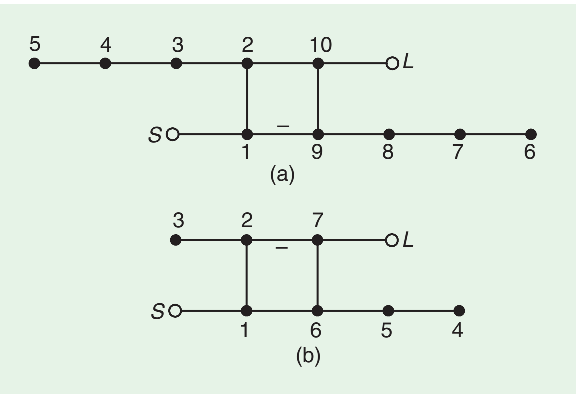

Figure 12. *Cul-de-Sac network configurations: (a) tenth degree (7 TZs max) and (b) seventh degree (4 TZs max) [24].*

configuration. An example of an odd degree characteristic is shown in Figure 12(b) (seventh-degree).

To transform the folded coupling matrix to the cul-de-sac form, a series of rotations is applied according to the following procedure:

For N even and $r = 1, 2, 3, \ldots, (N-2)/2$:
For rotation # r:

Pivot of rth rotation $= [i, j]$ where $i = (N+2)/2 - r$ and $j = N/2 + r$

$$\text{Angle} = \theta_r = \frac{1}{2}\tan^{-1}\left(\frac{2M_{ij}}{(M_{jj} - M_{ii})}\right) \text{ (cross-pivot rotation)} \tag{10a}$$

For N odd and $r = 1, 2, 3, \ldots, (N-3)/2$
For rotation # r:

Pivot of rth rotation $= [i, j]$ where $i = (N+1)/2 - r$ and $j = (N+1)/2 + r$

$$\text{Angle} = \theta_r = \tan^{-1}(M_{i,j-1}/M_{j-1,j}) \tag{10b}$$

For example, for a seventh-degree filtering function with three TZs:
Number of rotations = 2
Rotation 1: $i = 3$ $j = 5$, therefore pivot 1 = [3, 5] and angle $\theta_1 = \tan^{-1}(M_{34}/M_{45})$
Rotation 2: $i = 2$ $j = 6$, therefore pivot 2 = [2, 6] and angle $\theta_2 = \tan^{-1}(M_{25}/M_{56})$

Figure 13 shows a realization in coaxial resonator technology, firstly configured in folded form (a) and after reconfiguration to the cul-de-sac form (b). In the cul-de-sac form all the couplings will of the same sign except for one in the central core quartet—which one is arbitrary. Also for this case where the number of TZs is less than the maximum permissible, all the couplings between resonators in the core quartet have the same absolute value.

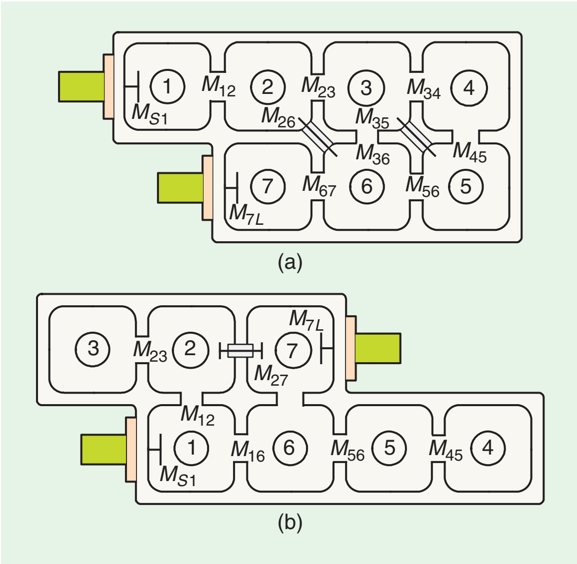

Figure 13. *7-1-2 asymmetric filter example—coaxial cavity realizations: (a) folded network configuration and (b) cul-de-sac configuration. (Reprinted with permission from [22].)*

Alternative Cul-de-Sac Configurations

In some cases it may give a more convenient configuration and better input-output isolation if the final rotation in the sequence is omitted. Such an example is shown in Figure 14(a) for an eighth-degree example, which gives a convenient rectangular topology and at least five resonators between input and output as compared with the basic cul-de-sac. It should be noted however that this topology will realize two fewer TZs than the basic version.

If the sequence is continued on for one further rotation than the basic sequence, the input and output couplings will be included in the core quartet as shown in Figure 14(b) for the eighth-degree example. This will realize two more TZs than the basic cul-de-sac (i.e., seven for this eighth-degree prototype), but if it is convenient to include the source-load coupling M_{SL} as shown in Figure 14(b), then all eight TZs may be realized (fully canonical network). If the original prototype

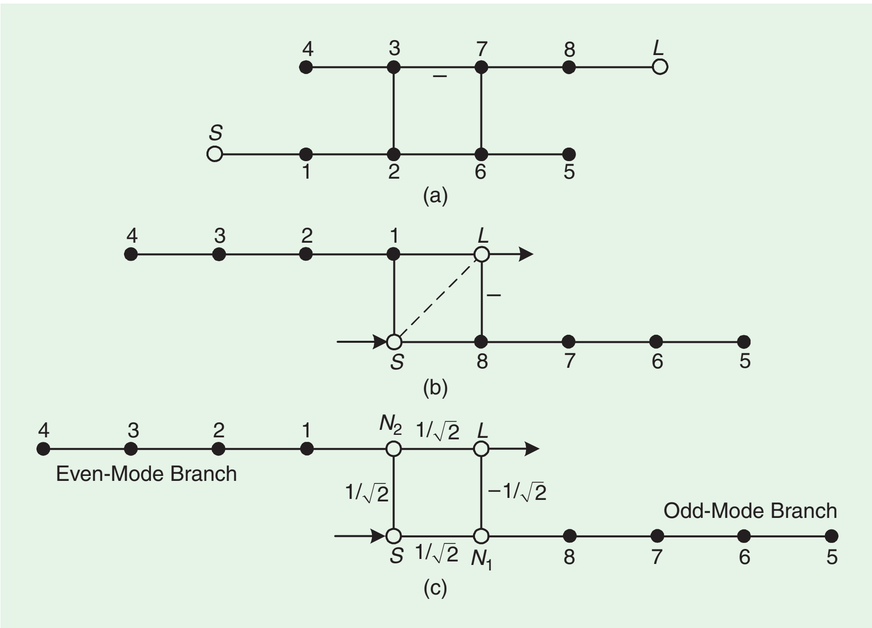

Figure 14. *Three alternative forms for the cul-de-sac configuration: (a) indirect-coupled, (b) fully canonical form, and (c) rat-race coupled even- and odd-mode networks. (Reprinted with permission from [22].)*

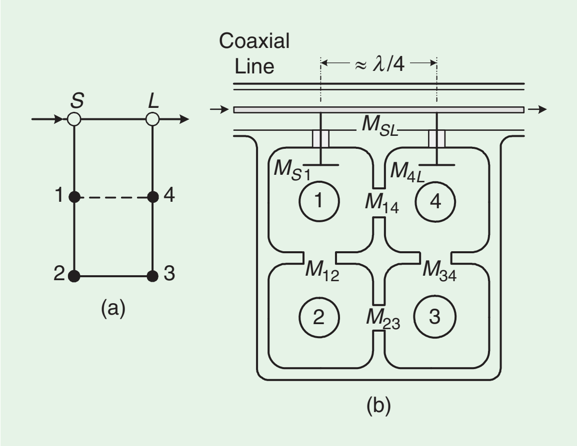

Figure 15. *4-2 Direct-coupled bandstop filter: (a) coupling and routing diagram and (b) possible realization with coaxial cavities. (Reprinted with permission from [22].)*

characteristic is fully canonical and M_{SL} is present in the original folded matrix, its value or position will not be changed by the cul-de-sac rotation sequence.

If an extra unity coupling inverter is added at each of the input and output ports so creating an $N+4$ matrix (the additional inverters will have no effect on S_{11} and S_{21} except to change their phases by 180°), and then the sequence is continued for yet another rotation, a situation arises where all four nodes in the core quartet are nonresonant, as shown in Figure 14(c). The values of the couplings in the core quartet will be $1/\sqrt{2}$, and together with the negative sign it becomes evident that the core is a rat-race coupler. This is easily realized in microstrip where the negative branch is realized with a 270° length of line instead of 90°. Also, the two branches of the network will have become the even mode and odd mode networks of the filtering function [30], [32], all synthesized quite automatically by the cul-de-sac procedure.

There are many advantages to be gained by using the cul-de-sac configuration, e.g., minimal number of couplings, no diagonal couplings even with asymmetric characteristics, convenient and flexible (even 3-D) layout possibilities. However the simple topology tends to produce a rather sensitive device in practice.

Bandstop Filters

To generate a bandstop characteristic from the regular low-pass prototype polynomials it is only necessary to exchange the reflection and transfer functions (including the constants) [22]:

$$S_{11}(s) = \frac{P(s)/\varepsilon}{E(s)} \qquad S_{21}(s) = \frac{F(s)/\varepsilon_R}{E(s)}. \tag{11}$$

Since $S_{21}(s)$ and $S_{11}(s)$ share a common denominator polynomial $E(s)$, the unitary conditions for a passive lossless network are preserved. If the characteristics are Chebyshev, then the original prescribed equiripple return loss characteristic becomes the transfer response, with a minimum reject level equal to the original prescribed return loss level. Because the degree of the new numerator polynomial for $S_{21}(s)$ $(=F(s)/\varepsilon_R)$ is now the same as its denominator $E(s)$, the network that is synthesized will be fully canonical. The new numerator of $S_{11}(s)$ is the original transfer function numerator polynomial $P(s)/\varepsilon$ and may have any number n_{fz} of prescribed TZs provided $n_{fz} \leq N$, the degree of the characteristic. If $n_{fz} < N$, then the constant $\varepsilon_R = 1$.

The network synthesis methods that have already been described may be used, once the $S_{21}(s)$ and $S_{11}(s)$ functions have been exchanged, to create a bandpass-like filter configuration but giving bandstop filter characteristics. The resonant cavities are direct-coupled so wideband performance is potentially better, and because the cavities are tuned to frequencies within the stopband, the main signal power will mainly route through the direct input-output coupling, bypassing the resonators and giving minimal insertion loss and relatively high power handling. An example of a fourth-degree bandstop filter realizing two symmetric reflection zeros (formerly TZs) is shown in Figure 15. If the original characteristic is to be asymmetric, then extra diagonal cross-couplings will be necessary, e.g., M_{13}.

Cul-de-Sac Forms for the Direct-Coupled Bandstop Matrix

If the number of reflection zeros of the bandstop characteristic is less than the degree of the network ($n_{fz} < N$ as above), and the network is double-terminated between equal source and load terminations, then a cul-de-sac form for the bandstop network, similar to that for bandpass filters, may be obtained by introducing two unity-impedance 45° phase lengths at either end of the network. This is equivalent to multiplying the $F(s)$, $F_{22}(s)$ and $P(s)$ polynomials by j, which has no effect on the overall transfer and reflection responses of the network apart from the 90° phase changes.

Synthesizing the network using the same methods as for a folded bandpass filter yields networks such as shown in Figure 16. These networks are characterized by

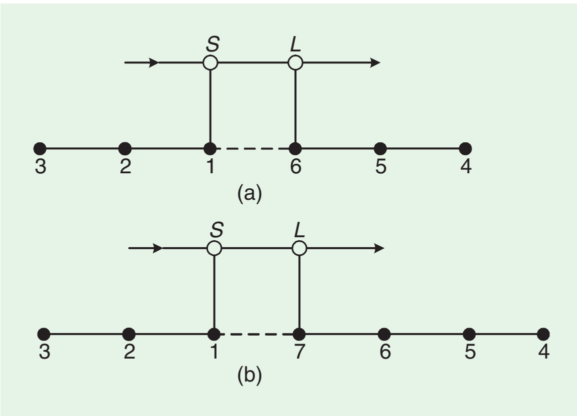

Figure 16. *Cul-de-sac forms for direct-coupled bandstop filters: (a) sixth degree and (b) seventh degree. (Reprinted with permission from [22].)*

the square-shaped core quartet of couplings, with the source and load terminals at adjacent corners at the input/output end, while the other resonators are strung out in two chains from the other two corners, in equal numbers if N is even and one more than the other if N is odd. There are no diagonal couplings even for asymmetric characteristics, and all couplings are of the same sign. For these characteristics where $n_{fz} < N$, the direct source-load coupling M_{SL} will always be unity in value. Figure 16 shows the coupling and routing diagrams of sixth- and seventh-degree examples.

Realization becomes particularly simple for this form of bandstop filter; an example of a four-two asymmetric bandstop filter is shown in Figure 17. This is the same low-pass prototype that was given as an example for a bandpass filter above, but note that the S_{21} and S_{11}characteristics have exchanged such that the in-band equiripple insertion loss is 22 dB (formerly the in-band equiripple return loss level for this prototype), and the out-of-stopband return loss lobe level is 30 dB on the upper side (formerly the rejection lobe level).

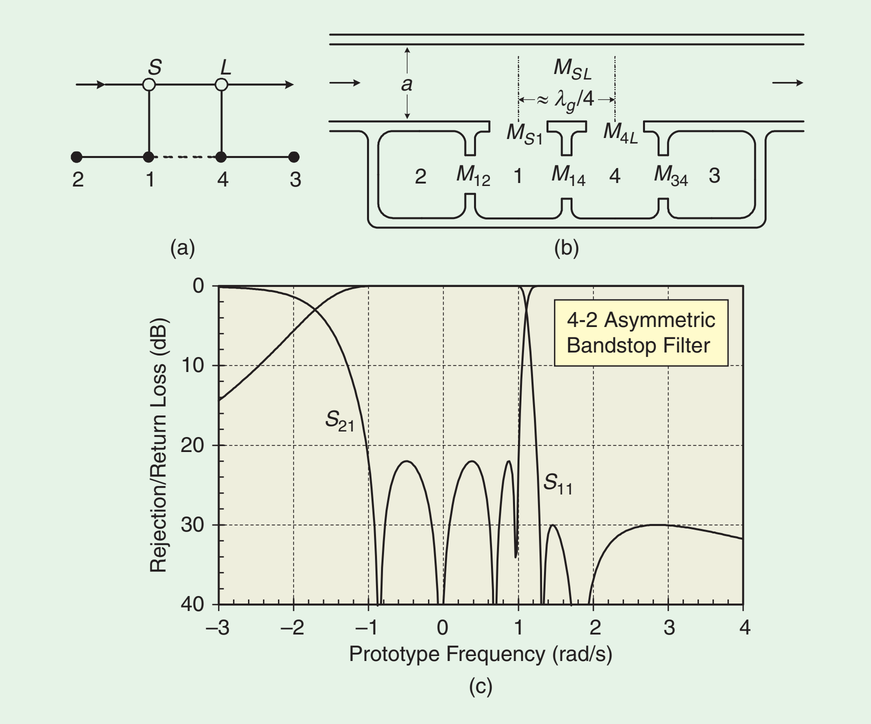

Figure 17. *4-2 Direct-coupled cul-de-sac bandstop filter: (a) coupling and routing diagram, (b) possible realization with waveguide cavities, (c) rejection and return loss performance. (Reprinted with permission from [22].)*

The bandstop filter may also be synthesized as the even mode and odd mode networks of the low-pass prototype attached to the branches of a coupler. It can be shown [32] that if the coupler network is configured as a 3 dB hybrid coupler, instead of a rat race coupler as for the bandpass filter, then the bandstop equivalent response will be obtained (i.e., the S_{21} and S_{11} responses exchange). The procedure is simply to first generate the $N+4$ rat-race-coupled bandpass cul-de-sac coupling matrix as described above and then to replace the elements of the rat-race coupler with those of the 3 dB hybrid coupler as shown in Figure 18, i.e., $M_{S,L} = M_{N1,N2} = 1$, $M_{S,N1} = M_{N2,L} = \sqrt{2}$. There is no need to change the values of the even-mode and odd-mode networks. Again this configuration is particularly suitable for realization in a planar technology, e.g., microstrip [30].

Trisections

A trisection comprises three couplings between three sequentially numbered nodes of a network, the first and third of which may be source or load terminals, or it might be embedded within the coupling matrix of a higher-degree network [34]–[36]. The minimum path rule indicates that trisections are able to realize one TZ each. As will be shown later, trisections may be merged using rotations to form higher order sections e.g., a quartet capable of realizing two TZs may be formed by merging two trisections.

Figure 19 shows four possible configurations. Figure 19(a) is an internal trisection, while Figure 19(b) and (c) shows input and output trisections respectively, where one node is the source or load termination. When the first and third nodes are the source and load terminations respectively [Figure 19(d)], we have a canonical network of degree 1 with the direct source-load coupling M_{SL} providing the single TZ. Trisections may also be cascaded with other trisections, either separately or conjoined [Figure 19(e) and (f)].

Being able to realize just one TZ each, the trisection is very useful for the synthesis of filters with asymmetric characteristics. They may exist singly within a network or multiply as a cascade. Rotations may be applied to reposition them along the diagonal of the overall coupling

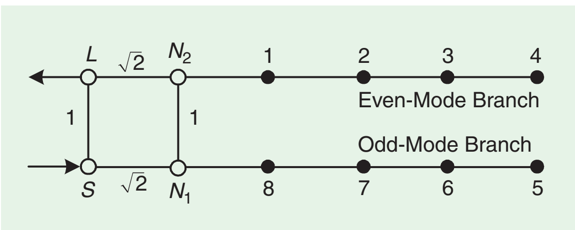

Figure 18. *Eighth-degree bandstop filter—synthesized as hybrid-coupled even-mode and odd-mode networks.*

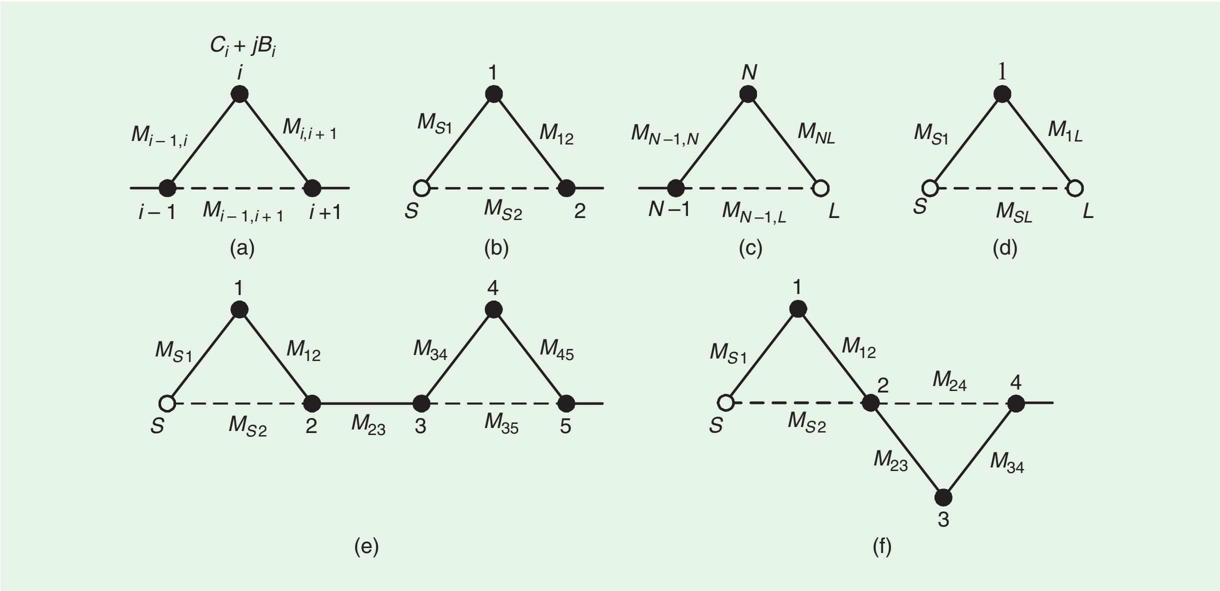

Figure 19. *Coupling and routing diagrams for trisections: (a) internal, (b) source-connected, (c) load-connected (d) canonical, (e) nonconjoined cascaded, (f) conjoined-cascaded. (Reprinted with permission from [22].)*

matrix, or to merge them to create quartet sections (two trisections) or quintet sections (three trisections), etc. Following on below an efficient procedure for synthesizing a cascade of trisections will be outlined [37].

Synthesis of the Arrow Canonical Coupling Matrix

The folded cross-coupled circuit and its corresponding coupling matrix was introduced above as one of the basic canonical forms of the coupling matrix, capable of realizing N TZs in an Nth-degree network. A second form was introduced by Bell [25] in 1982, which later become known as the wheel or arrow form. As with the folded form, all the main-line couplings are present, and in addition the source terminal and each resonator node is cross-coupled to the load terminal.

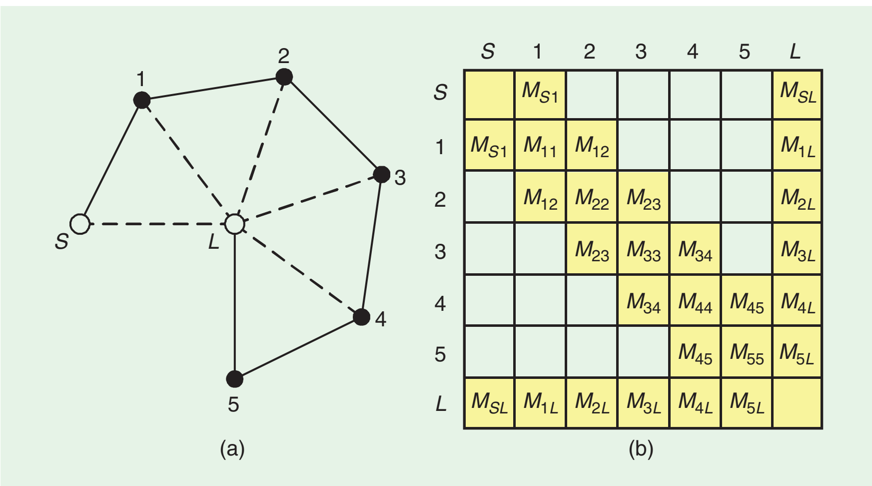

Figure 20. *Fifth-degree wheel or arrow canonical circuit. (a) Coupling and routing diagram (wheel). (b) N+2 coupling matrix (arrow). (Reprinted with permission from [22].)*

Figure 20(a) gives an example of the coupling and routing diagram for a fifth-degree fully canonical filtering circuit, showing clearly why this configuration is referred to as the wheel, with the main-line couplings forming the (partially incomplete) rim and the cross-couplings and input/output coupling forming the spokes. Figure 20(b) shows the corresponding coupling matrix where the cross-coupling elements are all in the last row and column, and together with the main line and self couplings on the main diagonals, give the matrix the appearance of an arrow pointing downwards towards the lower right corner of the matrix. The arrow matrix may be synthesized from the canonical transversal matrix with a formal sequence of rotations, similar to that for the folded matrix [22].

The basis of the trisection synthesis procedure relies on the fact that the value of the determinant of the self and mutual couplings of the trisection evaluated at $\omega = \omega_0$, the position of the TZ associated with the trisection, is zero:

$$\det\begin{vmatrix} M_{k-1,k} & M_{k-1,k+1} \\ \omega_0 + M_{k,k} & M_{k,k+1} \end{vmatrix} = 0 \tag{12}$$

where k is the number of the middle resonator of the trisection.

Figure 21 gives the topology and coupling matrix for the fourth-degree filter with 22 dB return loss and two TZs at $\omega_{01} = 1.8082$ and $\omega_{02} = 1.3217$ that was used as an example

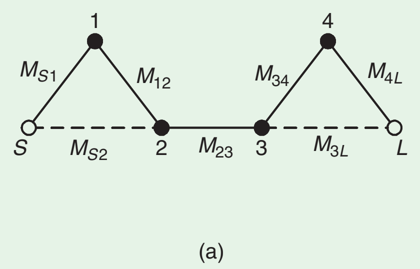

Trisection S-1-2 (ω_{01}) Trisection 3-4-L (ω_{02})

	S	1	2	3	4	L
S	0.0	0.9221	0.5921	0	0	0
1	0.9221	–0.8333	0.6259	0	0	0
2	0.5921	0.6259	0.6022	0.8634	0	0
3	0	0	0.8634	0.5812	0.2590	0.8471
4	0	0	0	0.2590	–1.1092	0.6952
L	0	0	0	0.8471	0.6952	0.0

(b)

Figure 21. *Fourth-degree filter with two transmission zeros realized as trisections. (a) Coupling/routing diagram. (b) Coupling matrix. (Reprinted with permission from [22].)*

earlier, now configured with two trisections to realize the two TZs. The shaded areas in the matrix indicate the couplings associated with each trisection.

Once the arrow coupling matrix has been formed, the procedure to create the first trisection realizing the first TZ at $\omega = \omega_{01}$ begins with conditioning the matrix with the application of a rotation at pivot $[N-1, N]$ and an angle θ_{01} to the original arrow matrix $\mathbf{M}^{(0)}$.

The rotation angle θ_{01} is given by (13):

$$\theta_{01} = \tan^{-1}\left[\frac{M^{(0)}_{N-1,N}}{\omega_{01} + M^{(0)}_{N,N}}\right] \tag{13}$$

where the superfix (0) indicates that the coupling values are taken from the original arrow matrix $\mathbf{M}^{(0)}$. The trisection may then be pulled up the diagonal of the matrix with further rotations such as pivot $[N-2, N-1]$ and angle $\theta_{12} = \tan^{-1}(M^{(1)}_{N-2,N}/M^{(1)}_{N-1,N})$ until it is in its desired position. The procedure is illustrated in Figure 22 for an asymmetric eighth degree example with four TZs.

Now the process may be repeated for the second trisection at $\omega = \omega_{02}$, and so on until a cascade of trisections is formed, one for each of the TZs in the original prototype, as shown in Figure 23(a). The trisections may be realized directly if it is convenient to do so, e.g.,

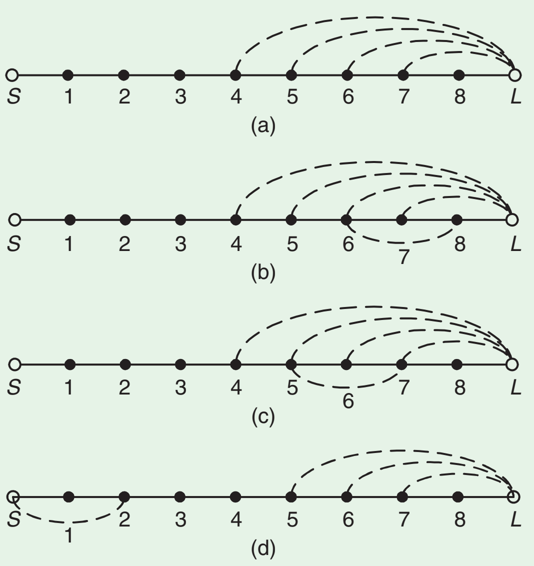

Figure 22. *8-2-2 synthesis example. (a) Coupling and routing diagram of initial arrow coupling matrix. (b) Conditioning rotation creates first trisection 6-7-8. (c) Rotation 2 pulls the trisection to position 5-6-7 … etc. (d) Rotation 7 finally creates trisection S-1-2. Note that when the trisection is in its final position, the outer cross coupling of the arrow formation (M_{4L}) automatically disappears. (Reprinted with permission from [22].)*

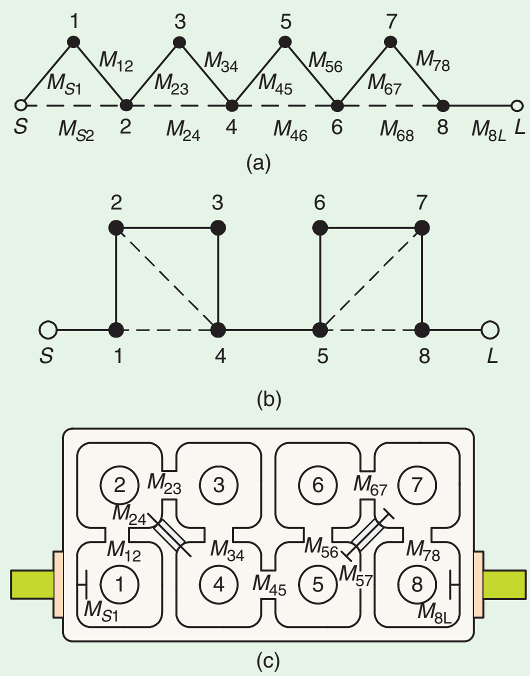

Figure 23. *8-4 asymmetric filter. (a) Trisection cascade. (b) Merging of trisections. (c) Coaxial resonator realization. Trisections S-1-2 and 2-3-4 merged to form quartet 1-2-3-4. Trisections 4-5-6 and 6-7-8 merged to form quartet 5-6-7-8. (Reprinted with permission from [22].)*

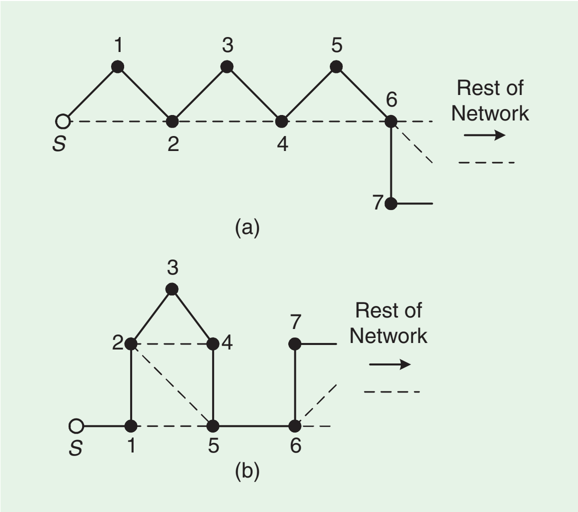

Figure 24. *Transformation of three conjoined trisections to form a quintet section. (a) Three cascaded trisections. (b) Trisections merged to form quintet. (Reprinted with permission from [22].)*

coupled coaxial resonators, but for other technologies such as dual-mode waveguide a cascade of quartets may be more suitable. This is easily achieved by merging adjacent trisections, as illustrated in Figure 23(b). If the two trisections being merged are realizing TZ pairs symmetrically located on the real or imaginary axes, or in quartets with symmetry about both axes, then the diagonal couplings [M_{24} and M_{57} in Figure 23(b)] will be zero. It is essential that complex zeros are in paraconjugate pairs, otherwise unrealizable complex coupling values will result. Figure 23(c) shows a possible coaxial-resonator realization for the two quartets.

This procedure may be extended to form even higher order sections in cascade, for example three trisections may be merged to form a quintet section, as illustrated in Figure 24.

Dual Band Symmetric Filter

An interesting configuration possibility arises if there are an odd number of TZs in a symmetric characteristic. For a single band filter this is anachronistic, since symmetry implies even numbers of TZs equally distributed above and below the passband. However a possibility arises with symmetric dual band filters, where one or more of the zeros is at zero frequency. Dual band filters have been finding application recently for suppressing interference between two closely spaced channels, for example.

	S	1	2	3	4	5	6	7	8	9	10	L
S	0	0.8388	0	0	0	0	0	0	0	0	0	0
1	0.8388	0	0.7144	0	–0.3894	0	0	0	0	0	0	0
2	0	0.7144	0	0.7832	0	0	0	0	0	0	0	0
3	0	0	0.7832	0	0.5052	0	0	0	0	0	0	0
4	0	–0.3894	0	0.5052	0	0.4423	0	0	0	0	0	0
5	0	0	0	0	0.4423	0	0.5174	0.4206	0	0	0	0
6	0	0	0	0	0	0.5174	0	0	0	0	0	0
7	0	0	0	0	0	0.4206	0	0	0.4574	0	–0.7156	0
8	0	0	0	0	0	0	0	0.4574	0	0.1590	0	0
9	0	0	0	0	0	0	0	0	0.1590	0	0.3871	0
10	0	0	0	0	0	0	0	–0.7156	0	0.3871	0	0.8388
L	0	0	0	0	0	0	0	0	0	0	0.8388	0

(a)

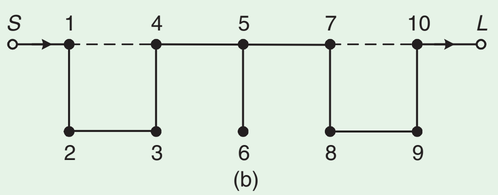

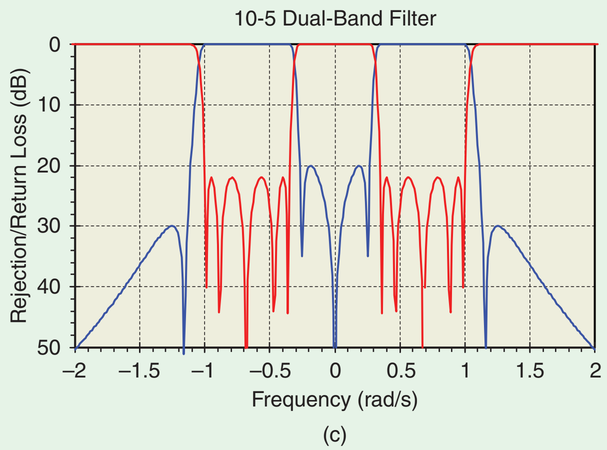

Figure 25. *Tenth-degree symmetric dual-band filter. (a) Coupling matrix. (b) Coupling/routing diagram. (c) Rejection/return loss performance.*

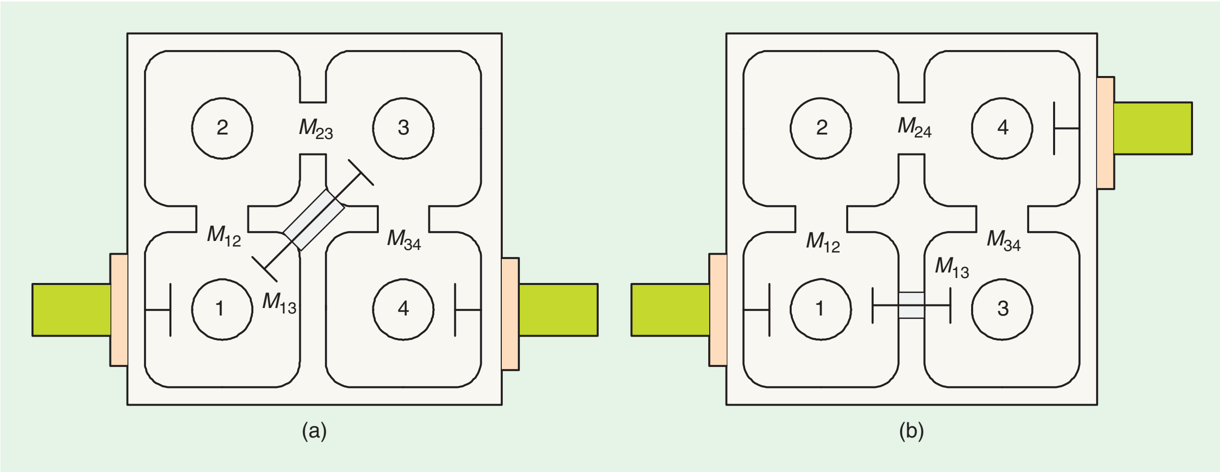

Figure 26. *4-1 asymmetric filtering function. (a) Realized with conventional diagonal cross coupling (M_{13}). (b) Realized with the box configuration [33].*

A case is taken of a symmetric dual-band prototype where the lower band lies between $\omega = -1.0$ and -0.35, the upper band between $\omega = +0.35$ and $+1.0$, two TZs are positioned on the outer sides of the two bands producing rejection lobes of 30 dB, and three between the bands (one at $\omega = 0$) producing lobes of 20 dB. The in-band return loss level is 22 dB.

If the network is synthesized as a series of trisections, and the complementary pairs combined to form two symmetric quartets, the remaining trisection 5-6-7 realizing the TZ at zero will have one of its main-line couplings missing, M_{67} in this case. Figure 25 shows the synthesized coupling matrix with the extracted zero resonator in the centre, although it does not necessarily have to be in that position. If there is more than one TZ at zero frequency, they too may be synthesized as extracted zeros.

Box and Extended Box Sections

The trisection may also be used to create another class of configuration known as the box or extended box class [33]. The box section is similar to the cascade quartet section, i.e., four resonator nodes arranged in a square formation; however with the input to and the output from the quartet from opposite corners of the square. Figure 26(a) shows the conventional quartet arrangement for a fourth degree filtering characteristic with a single TZ, realized with a trisection. Figure 26(b) shows the equivalent box section realizing the same TZ but without the need for the diagonal coupling. Application of the minimum path rule indicates that the box section can realize only a single TZ.

The box section is created by the application of a cross-pivot rotation (as used with cul-de-sac filter synthesis) to a trisection that has been synthesized within the overall coupling matrix for the filter. To transform the trisection into a basic box section, the rotation pivot is set to annihilate the second main line coupling of the trisection in the coupling matrix, i.e., pivot = [2, 3] annihilating element M_{23} [cross-pivot rotation, see (10a)] in the trisection 1-2-3 in the fourth degree example of Figure 26(a) and its equivalent coupling and routing schematic Figure 27(a). In the process of annihilating the main line coupling M_{23}, the coupling M_{24} is created [Figure 27(b)], and then by untwisting the network the box section is formed [Figure 27(c)].

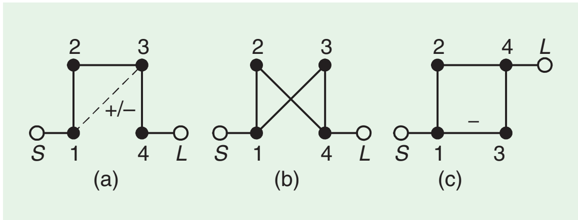

Figure 27. *4-1 filter—formation of the box section. (a) Trisection. (b) Annihilation of M_{23} and creation of M_{24}. (c) Untwisting to obtain box section [33].*

In the resultant box section, one of the couplings will always be negative, irrespective of the sign of the cross-coupling (M_{13}) in the original trisection. Figure 28(a) gives the coupling and routing diagram for a tenth degree example with two TZs realized as trisections and where each trisection has been transformed into a box section within the matrix by the application of two cross-pivot rotations at pivots [2, 3] and [8, 9] [Figure 28(b)]. Having no diagonal couplings, this form is suitable for realization in dual-mode technology.

An interesting feature of the box section is that to create the complementary response (i.e., the TZ appears on the opposite side of the passband), it is only necessary to change the values of the self couplings to their conjugate values. In practice this is a process of retuning the resonators of the RF device—no couplings need to be changed in value or sign. This means that the same physical structure may be used for the filters of a complementary diplexer, for example.

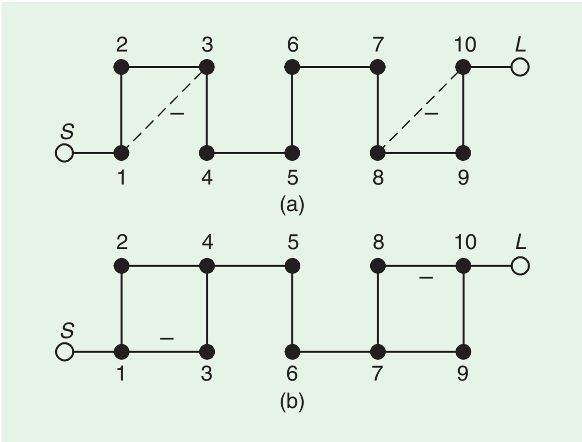

Figure 28. *10-2 asymmetric filter—coupling and routing diagrams. (a) Synthesized with two trisections. (b) After transformation of trisections to two box sections [33].*

Extended Box Sections

The basic box section may be extended to enable a greater number of TZs to be realized, but retaining a convenient physical arrangement, as shown in Figure 29 [33]. Here the basic fourth degree box section is shown and then the addition of pairs of resonators to form sixth, eighth and tenth degree networks. Application of the minimum path rule indicates that a maximum of $1, 2, 3, 4, \ldots, (N-2)/2$ TZs may be realized by the 4th, 6th, 8th, 10th, ..., Nth-degree networks respectively. The resonators are arranged in two parallel rows with half the total number of resonators in each row, input is at the corner at one end and output from the diagonally opposite corner at the other end. Even though asymmetric characteristics may be prescribed, there are no diagonal cross-couplings.

There appears to be no regular pattern for determining the sequence of rotations to synthesize the coupling matrix for the extended box sections from the folded network or any other canonical network. The networks may be synthesized using optimization techniques [22], [38], [39], but more recently a procedure [40] based on the use of the Groebner basis to solve nonlinear equations has become available through the software package Dedale-HF, which is accessible on the Internet [41].

An interesting feature of extended box filters is that multiple solutions for the coupling matrices exist for the same prototype filtering characteristic. This means that optimal coupling matrix values may be chosen for the RF technology it is intended to realize the extended box filter with. The number of real solutions depends on the degree and TZ pattern of the filtering function, e.g., 16 for an eighth degree and 58 for a tenth degree characteristic. The multiple solution feature however can cause a problem when trying to de-embed coupling values from a measured performance.

Conclusions

In this article, some of the more recent developments in the art of filter synthesis have been outlined. These have been mainly based on the coupling matrix representation of the filter's coupling arrangements, because of the amenity of the coupling matrix to mathematical manipulation, and the one-to-one correspondence of the elements of the coupling matrix to the real filter parameters.

The methods described in this article probably do not cover all those available today for filter network synthesis. It is known that some advanced research work is ongoing into the synthesis of lossy filters [42]–[47] which are used to compensate for a low resonator Q and give very linear in-band performance but at the expense of a high-ish insertion loss (not a real problem in low-power circuits). Also, some work is ongoing into the synthesis of coupling matrices for wideband devices, where the coupling elements have a frequency dependency [48]. Some novel synthesis techniques have recently come available for the design of circuits incorporating the nonresonant node (NRN) element, which are useful in high power applications and for easing the design of dielectric and planar circuits [49]–[51].

The Dedale-HF CAD package mentioned above for creating extended box solutions may also be used to solve other topological cases which are not amenable to a series of analytical transformations, and which can only be solved with an optimization approach. Another CAD optimization procedure known as space mapping has also become available recently, and has been widely used for the design of complex filters and multiplexers [52].

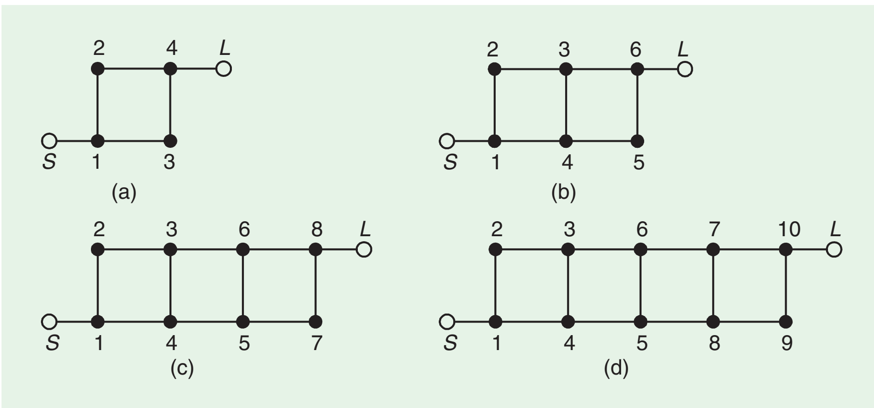

Figure 29. *Coupling and routing diagrams for extended box section networks. (a) fourth-degree (basic box section). (b) sixth-degree. (c) eighth-degree. (d) tenth-degree.*

References

[1] O. Brune, "Synthesis of a finite 2-terminal network whose driving point impedance is a prescribed function of frequency," *J. Math. Phys.*, vol. 10, no. 3, pp. 191–236, 1931.

[2] S. Darlington, "Synthesis of reactance 4-poles which produce insertion loss characteristics," *J. Math. Phys.*, vol. 18, pp. 257–353, 1939.

[3] H. W. Bode, *Network Analysis and Feedback Amplifier Design*. Princeton, NJ: Van Nostrand, 1945.

[4] M. E. van Valkenburg, *Network Analysis*. Englewood Cliffs, NJ: Prentice-Hall, 1955.

[5] H. J. Carlin, "The scattering matrix in network theory," *IRE Trans. Circuit Theory*, vol. CT-3, pp. 88–96, June 1956.

[6] R. F. Baum, "Design of unsymmetrical band-pass filters," *IRE Trans. Circuit Theory*, vol. CT-4, pp. 33–40, June 1957.

[7] S. B. Cohn, "Direct coupled cavity filters," *Proc. IRE*, vol. 45, pp. 187–196, Feb. 1957.

[8] E. A. Guillemin, *Synthesis of Passive Networks*. New York: Wiley, 1957.

[9] W. Cauer, *Synthesis of Linear Communication Networks*. New York: McGraw-Hill, 1958.

[10] R Saal and E. Ulbrich, "On the design of filters by synthesis," *IRE Trans.*, vol. CT-5, pp. 284–327, Dec. 1958.

[11] G. Matthaei, L. Young, and E. M. T. Jones, *Microwave Filters, Impedance Matching Networks and Coupling Structures*. Norwood, MA: Artech House, 1980.

[12] R. Levy, "Theory of direct coupled cavity filters," *IEEE Trans. Microwave Theory Tech.*, vol. 11, pp. 162–178, May 1963.

[13] H. J. Orchard and G. C. Temes, "Filter design using transformed variables," *IEEE Trans. Circuit Theory*, vol. CT-15, pp. 385–408, Dec. 1968.

[14] J. D. Rhodes, *Theory of Electrical Filters*. New York: Wiley, 1976.

[15] J. D. Rhodes, "Filters approximating ideal amplitude and arbitrary phase characteristics," *IEEE Trans. Circuit Theory*, vol. 20, pp. 150–153, Mar. 1973.

[16] J. D. Rhodes, "The generalized direct-coupled cavity linear phase filter," *IEEE Trans. Microwave Theory Tech.*, vol. 18, pp. 308–313, June 1970.

[17] A. E. Atia and A. E. Williams, "New types of bandpass filters for satellite transponders," *COMSAT Tech. Rev.*, vol. 1, pp. 21–43, Fall 1971.

[18] A. E. Atia and A. E. Williams, "Narrow-bandpass waveguide filters," *IEEE Trans. Microwave Theory Tech.*, vol. 20, pp. 258–265, Apr. 1972.

[19] A. E. Atia and A. E. Williams, "Nonminimum-phase optimum-amplitude bandpass waveguide filters," *IEEE Trans. Microwave Theory Tech.*, vol. 22, pp. 425–431, Apr. 1974.

[20] A. E. Atia, A. E. Williams, and R. W. Newcomb, "Narrow-band multiple-coupled cavity synthesis," *IEEE Trans. Circuits Syst.*, vol. 21, pp. 649–655, Sept. 1974.

[21] R. J. Cameron, "General coupling matrix synthesis methods for Chebyshev filtering functions," *IEEE Trans. Microwave Theory Tech.*, vol. 47, pp. 433–442, Apr. 1999.

[22] R. J. Cameron, C. M. Kudsia, and R. R. Mansour, *Microwave Filters for Communication Systems, Fundamentals, Design and Applications*. New York: Wiley, 2007.

[23] J. D. Rhodes and S. A. Alseyab, "The generalized Chebyshev low-pass prototype filter," *IEEE Trans. Circuit Theory*, vol. 8, pp. 113–125, 1980.

[24] R. J. Cameron, "Advanced coupling matrix synthesis techniques for microwave filters," *IEEE Trans. Microwave Theory Tech.*, vol. 51, pp. 1–10, Jan. 2003.

[25] H. C. Bell, "Canonical asymmetric coupled-resonator filters," *IEEE Trans. Microwave Theory Tech.*, vol. 30, pp. 1335–1340, Sept. 1982.

[26] F. R. Gantmacher, *The Theory of Matrices*, vol. 1. New York: Chelsea, 1959.

[27] J. D. Rhodes, "A low-pass prototype network for microwave linear phase filters," *IEEE Trans. Microwave Theory Tech.*, vol. 18, pp. 290–300, June 1970.

[28] R. J. Cameron, "A novel realization for microwave bandpass filters," *ESA J.*, vol. 3, pp. 281–287, 1979.

[29] R. J. Cameron and J. D. Rhodes, "Asymmetric realizations for dual-mode bandpass filters," *IEEE Trans. Microwave Theory Tech.*, vol. 29, pp. 51–58, Jan. 1981.

[30] I. C. Hunter, *Theory and Design of Microwave Filters (Electromagnetic Waves Series 48)*. London: IEE, 2001.

[31] G. Pfitzenmaier, "An exact solution for a six-cavity dual-mode elliptic bandpass filter," in *IEEE MTT-S Int. Microwave Symp. Dig.*, San Diego, CA, 1977, pp. 400–403.

[32] W. M. Fathelbab, "Synthesis of Cul-de-Sac filter networks utilizing hybrid couplers," *IEEE Microwave Wireless Comp. Lett.*, vol. 17, no. 5, pp. 334–336, May 2007.

[33] R. J. Cameron, A. R. Harish, and C. J. Radcliffe, "Synthesis of advanced microwave filters without diagonal cross-couplings," *IEEE Trans. Microwave Theory Tech.*, vol. 50, pp. 2862–2872, Dec. 2002.

[34] R. J. Cameron, "General prototype network synthesis methods for microwave filters," *ESA J.*, vol. 6, pp. 193–206, 1982.

[35] R. Levy, "Filters with single transmission zeros at real or imaginary frequencies," *IEEE Trans. Microwave Theory Tech.*, vol. 24, pp. 172–181, Apr. 1976.

[36] R. Levy and P. Petre, "Design of CT and CQ filters using approximation and optimization," *IEEE Trans. Microwave Theory Tech.*, vol. 49, pp. 2350–2356, Dec. 2001.

[37] S. Tamiazzo and G. Macchiarella, "An analytical technique for the synthesis of cascaded N-tuplets cross-coupled resonators microwave filters using matrix rotations," *IEEE Trans. Microwave Theory Tech.*, vol. 53, pp. 1693–1698, May 2005.

[38] S. Amari, "Synthesis of cross-coupled resonator filters using an analytical gradient-based optimization technique," *IEEE Trans. Microwave Theory Tech.*, vol. 48, no. 9, pp. 1559–1564, Sept. 2000.

[39] W. A. Atia, K. A. Zaki, and A. E. Atia, "Synthesis of general topology multiple-coupled resonator filters by optimization," in *IEEE MTT-S Int. Microwave Symp. Dig.*, 1998, vol. 2, pp. 821–824.

[40] R. J. Cameron, J. C. Faugere, F. Roullier, and F. Seyfert, "Exhaustive approach to the coupling matrix synthesis problem and the application to the design of high degree asymmetric filters," *Int. J. RF Microwave Comput.-Aided Eng.*, vol. 17, no. 1, pp. 4–12, Jan. 2007.

[41] Dedale-HF page. [Online]. Available: http://www.sop-inria.fr/apics/Dedale

[42] M. Oldini, G. Macchierella, G. Gentili, and C. Ernst, "A new approach to the synthesis of microwave lossy filters," *IEEE Trans. Microwave Theory Tech.*, vol. 58, no. 5, pp. 1222–1229, May 2010.

[43] V. Miraftab and M. Yu, "Advanced coupling matrix and admittance function synthesis techniques for dissipative microwave filters," *IEEE Trans. Microwave Theory Tech.*, vol. 57, no. 10, pp. 2429–2438, Oct. 2009.

[44] J. D. Rhodes and I. C. Hunter, "Synthesis of reflection-mode prototype networks with dissipative circuit elements," *Proc. Inst. Elect. Eng.—Microwave, Antennas, Propagat.*, vol. 144, no. 6, pp. 437–442, Dec. 1997.

[45] W. Fathelbab, I. C. Hunter, and J. D. Rhodes, "Synthesis of lossy reflection mode prototype networks with symmetrical and asymmetrical characteristics," *Proc. Inst. Elect. Eng.—Microwave, Antennas, Propagat.*, vol. 146, no. 2, pp. 97–104, Apr. 1999.

[46] A. Guyette, I. Hunter, and R. Pollard, "The design of microwave bandpass filters using resonators with nonuniform Q," *IEEE Trans. Microwave Theory Tech.*, vol. 54, no. 11, pp. 3914–3922, Nov. 2006.

[47] I. C. Hunter, A. Guyette, and R. Pollard, "Passive microwave receive filter networks using low-Q resonators," *IEEE Microwave Mag.*, vol. 6, no. 3, pp. 1959–1962, Sept. 2005.

[48] S. Amari, F. Seyfert, and M. Bekheit, "Theory of coupled resonator microwave bandpass filters of arbitrary bandwidth," *IEEE Trans. Microwave Theory Tech.*, vol. 58, no. 8, pp. 2188–2203, Aug. 2010.

[49] S. Amari and U. Rosenberg, "New building blocks for modular deisgn of elliptic and self-equalized filters," *IEEE Trans. Microwave Theory Tech.*, vol. 52, pp. 721–736, Feb. 2004.

[50] S. Amari and U. Rosenberg, "A universal building block for advanced modular design of microwave filters," *IEEE Microwave Wireless Comp. Lett.*, vol. 13, pp. 541–543, Dec. 2003.

[51] D. C. Rebenaque, F. Q. Pereira, J. P. Garcia, A. A. Melcon, and M. Guglielmi, "Two compact configurations for implementing transmission zeros in microstrip filters," *IEEE Microwave Wireless Comp. Lett.*, vol. 14, pp. 475–477, Oct. 2004.

[52] J. W. Bandler, Q. S. Cheng, S. A. Dakroury, A. S. Mohamed, M. H. Bakr, K. Madsen, and J. Sondergaard, "Space mapping: The state-of-the-art," *IEEE Trans. Microwave Theory Tech.*, vol. 52, pp. 337–361, Jan. 2004.